Supplementary Material for "Large optical conductivity of Dirac semimetal Fermi arc surfaces states"

Dispersion and Location of Fermi arc states

The low energy effective Hamiltonian of 3D topological Dirac semimetal (DSM) in the bulk can be captured by a minimal 4×4 Hamiltonian $\mathcal{H}=\mathcal{H}_0+\mathcal{H}'$ with

$$\mathcal{H}_0 = m_{\mathbf{k}}\mathbf{s}_0\boldsymbol{\tau}_3 + v(k_x\mathbf{s}_3\boldsymbol{\tau}_1 - k_y\mathbf{s}_0\boldsymbol{\tau}_2), \tag{15}$$

and $\mathcal{H}' = \alpha k_z[(k_x^2-k_y^2)\mathbf{s}_1\boldsymbol{\tau}_1 - k_xk_y\mathbf{s}_2\boldsymbol{\tau}_1]$, where $\mathbf{k}=(k_x,k_y,k_z)$ is taken about the $\Gamma_{3\mathrm{D}}=(0,0,0)$ point, $\mathbf{s}_0$ ($\boldsymbol{\tau}_0$) is an identity matrix, $\mathbf{s}_{1,2,3}$ ($\boldsymbol{\tau}_{1,2,3}$) are Pauli matrices representing the spin (orbital) degrees of freedom, and α determines the magnitude of the high-order term $\mathcal{H}'$[1]. We note that m is a mass parameter that characterizes the band inversion of bands with different parity [1–3]. In three-dimensional topological Dirac semimetals, the crystal possesses rotational symmetry about the $\hat{\mathbf{z}}$ axis. Consequently, on the k_z axis the band inversion takes the form

$$m(k_x=0,k_y=0,k_z) = -m_0 + m_1k_z^2, \tag{16}$$

and $\mathcal{H}'=0$. Using this form of the band inversion captured in $m(0,0,k_z)$ in Eq. (15), a pair of Dirac points $(0,0,\pm k_0)$ with $k_0=\sqrt{m_0/m_1}$ emerge in the bulk due to the band inversion around the Γ point and rotational symmetry along the k_z axis.

We will now consider a semi-infinite DSM that fills $y>0$, and vacuum for $y<0$. This leaves a x-z surface at $y=0$. Note that in the DSM $m_0>0$ in Eq. (16) since bands with different parity are inverted close to Γ. As a result, we will model $m_0(y)>0$ for $y\geq0$ (for the DSM), and $m_0(y)<0$ when $y<0$ (for vacuum).

To obtain the Fermi arc surface states, we substitute

$$ik_y \to \partial_y \tag{17}$$

in the Hamiltonian $\mathcal{H}$ throughout and use an ansatz for the surface state wavefunction: $\Psi^{\mathrm{surf}}_{\mathbf{k}_{2\mathrm{D}}\uparrow\downarrow}(y) = \mathcal{N}^{-1}_{\mathbf{k}_{2\mathrm{D}}}e^{-y/\lambda_{\mathbf{k}_{2\mathrm{D}}}}u_{\uparrow\downarrow}$ which is localized at the surface at $y=0$ and decays in the bulk. Here $\mathbf{k}_{2\mathrm{D}}=(k_x,k_z)$ and $u_{\uparrow\downarrow}$ are a pair of k-independent and orthogonal spinors corresponding to the $s=1$ and $s=-1$ spin blocks in Eq. (15). Taking $\mathcal{H}'=0$ since it is weak and vanishes along the k_z axis as $\mathcal{H}'\sim\mathcal{O}(k^3)$, we obtain an eigenproblem for each of the spins. For spin $\uparrow$ ($\downarrow$) and using a y-position representation with the surface state wavefucntion ansatz above, we have

$$\begin{pmatrix} m_{\mathbf{k}_{2\mathrm{D}}}-\varepsilon_{\mathbf{k}_{2\mathrm{D}}} & \pm vk_x + v/\lambda_{\mathbf{k}_{2\mathrm{D}}} \\ \pm vk_x - v/\lambda_{\mathbf{k}_{2\mathrm{D}}} & -m_{\mathbf{k}_{2\mathrm{D}}}-\varepsilon_{\mathbf{k}_{2\mathrm{D}}} \end{pmatrix}\begin{pmatrix}\Psi^{\mathrm{surf}}_{1(3)}\\ \Psi^{\mathrm{surf}}_{2(4)}\end{pmatrix}=0, \tag{18}$$

where Ψ^{surf}_i represents the components of the 4-spinor $\Psi^{\mathrm{surf}} = (\Psi^{\mathrm{surf}}_{\mathbf{k}_{2\mathrm{D}},\uparrow},\Psi^{\mathrm{surf}}_{\mathbf{k}_{2\mathrm{D}},\downarrow})$; here $i=1,2,3,4$. Solving Eq. (18) yields Jackiw-Rebi type surface state wavefunctions ($\Psi^{\mathrm{surf}}_{\mathbf{k}_{2\mathrm{D}}\uparrow}(y) = \langle y|\Psi^{\mathrm{surf}}_{\mathbf{k}_{2\mathrm{D}}\uparrow}\rangle$) localized around $y=0$ which decays into the bulk ($y\geq0$):

$$\Psi^{\mathrm{surf}}_{\mathbf{k}_{2\mathrm{D}}\uparrow}(y) = \frac{e^{-y/\lambda_{\mathbf{k}_{2\mathrm{D}}}}}{\mathcal{N}_{\mathbf{k}_{2\mathrm{D}}}}\begin{pmatrix}1\\1\\0\\0\end{pmatrix},\quad \Psi^{\mathrm{surf}}_{\mathbf{k}_{2\mathrm{D}}\downarrow}(y) = \frac{e^{-y/\lambda_{\mathbf{k}_{2\mathrm{D}}}}}{\mathcal{N}_{\mathbf{k}_{2\mathrm{D}}}}\begin{pmatrix}0\\0\\1\\1\end{pmatrix}, \tag{19}$$

where the plane wave part, $e^{i(k_xx+k_zz)}$, is implicit, and $\mathcal{N}_{\mathbf{k}_{2\mathrm{D}}}$ the normalization constant. The energy and $\lambda_{\mathbf{k}_{2\mathrm{D}}}$ reads

$$\varepsilon_{\mathbf{k}_{2\mathrm{D}}\uparrow\downarrow} = \pm vk_x,\quad \lambda_{\mathbf{k}_{2\mathrm{D}}} = -v/m_{\mathbf{k}_{2\mathrm{D}}}. \tag{20}$$

We emphasize that $\lambda_{\mathbf{k}_{2\mathrm{D}}}=-v/m_{\mathbf{k}_{2\mathrm{D}}}$ is a self-consistent equation since the mass parameter itself depends on λ via $m(k_x,ik_y\to-1/\lambda_{\mathbf{k}_{2\mathrm{D}}},k_z)$.

When $m_{\mathbf{k}_{2\mathrm{D}}}\to0$, the decay length $\lambda_{\mathbf{k}_{2\mathrm{D}}}=-v/m_{\mathbf{k}_{2\mathrm{D}}}$ diverges and the wavefunction merges into the bulk. As a result, the positivity of the decay length, i.e., the normalizable requirement of the wavefunction, limits the existence of surface states in k-space to the region where $m_{\mathbf{k}_{2\mathrm{D}}}<0$. Therefore we can only find Fermi arc states between $k_z\in[-k_0,k_0]$ with $k_0=\sqrt{m_0/m_1}$, i.e., the two projected Dirac points $\pm\mathbf{k}^{\mathrm{Dirac}}_{2\mathrm{D}}=(k_x=0,k_z=k_0)$.

Effective Hamiltonian for the Surface States

To obtain the effective Hamiltonian for Fermi arc surface states, we use $|\Psi^{\mathrm{surf}}_{\mathbf{k}_{2\mathrm{D}}\uparrow\downarrow}\rangle$ as a basis and treat $\mathcal{H}'_{4\times4}$ as perturbation. Projecting the full 4×4 Hamiltonian into this basis, we obtain the surface Hamiltonian

$$[\mathcal{H}_{\mathrm{surf}}(\mathbf{k}_{2\mathrm{D}})]_{ij} = \langle\Psi^{\mathrm{surf}}_{\mathbf{k}_{2\mathrm{D}}i}|\mathcal{H}_0(\mathbf{k}_{2\mathrm{D}})+\mathcal{H}'(\mathbf{k}_{2\mathrm{D}})|\Psi^{\mathrm{surf}}_{\mathbf{k}_{2\mathrm{D}}j}\rangle,\quad (i,j=\uparrow\downarrow), \tag{21}$$

where $\mathbf{k}_{2\mathrm{D}}=(k_x,k_z)$, and the inner product is defined as

$$\begin{aligned}
&\langle\Psi^{\mathrm{surf}}_{\mathbf{k}_{2\mathrm{D}}i}|\hat{O}(\mathbf{k})|\Psi^{\mathrm{surf}}_{\mathbf{k}_{2\mathrm{D}}j}\rangle\\
=&\int_0^\infty dy\ [\Psi^{\mathrm{surf}}_{\mathbf{k}_{2\mathrm{D}}i}(y)]^*\hat{O}(\mathbf{k}_{2\mathrm{D}},ik_y\to\partial_y)\Psi^{\mathrm{surf}}_{\mathbf{k}_{2\mathrm{D}}j}(y)\\
=&u_i^TO(\mathbf{k}_{2\mathrm{D}},ik_y\to-1/\lambda_{\mathbf{k}_{2\mathrm{D}}})u_j\times\int_0^\infty dy\ \left(\frac{e^{-y/\lambda_{\mathbf{k}_{2\mathrm{D}}}}}{\mathcal{N}_{\mathbf{k}_{2\mathrm{D}}}}\right)^2\\
=&u_i^TO(\mathbf{k}_{2\mathrm{D}},ik_y\to-1/\lambda_{\mathbf{k}_{2\mathrm{D}}})u_j,
\end{aligned} \tag{22}$$

where we have used the normalization condition in the y-direction, and in writing the inner product we have used the y-position representation of the surface state wavefunction.

For Dirac semimetals with rotational symmetry, e.g., Cd_3As_2 (structure I) with 4-fold rotational symmetry

and A_3Bi (A=Na, K, Rb) with 3-fold rotational symmetry, to the lowest order of k^3,

$$\mathcal{H}' = \begin{pmatrix} 0 & 0 & 0 & B^*(\mathbf{k}) \\ 0 & 0 & B^*(\mathbf{k}) & 0 \\ 0 & B(\mathbf{k}) & 0 & 0 \\ B(\mathbf{k}) & 0 & 0 & 0 \end{pmatrix}, \tag{23}$$

where

$$B(\mathbf{k}) = \alpha k_z (k_x + i k_y)^2 \tag{24}$$

due to the conservation of the angular momentum, and α denotes the magnitude of this $\mathcal{O}(k^3)$ coupling.

Using the basis wavefunctions from the previous section and Eq. (22), one can verify that the effective surface Hamiltonian reads as

$$\mathcal{H}_{\text{surf},0} = v k_x \sigma_z + \Delta^{(0)}_{\mathbf{k}_{2\text{D}}} \sigma_x, \tag{25}$$

in which

$$\Delta^{(0)}_{\mathbf{k}_{2\text{D}}} = \langle \Psi^{\text{surf}}_{\mathbf{k}_{2\text{D}}\uparrow} | \mathcal{H}' | \Psi^{\text{surf}}_{\mathbf{k}_{2\text{D}}\downarrow} \rangle = \alpha k_z (k_x - 1/\lambda_{\mathbf{k}_{2\text{D}}})^2, \tag{26}$$

capturing the intrinsic coupling between the $\uparrow$ and $\downarrow$ surface states. Note that the inner product is defined in Eq. (22).

We note that $\Delta^{(0)}_{\mathbf{k}_{2\text{D}}}$ has three nodes: one node at $\mathbf{k}_{2\text{D}} = (0,0)$, and a pair at the projected Dirac points $\pm\mathbf{k}^{\text{Dirac}}_{2\text{D}} = (k_x = 0, k_z = \pm k_0)$. The former node, arises from a Kramers degeneracy of spin up and down surface states at the projected $\mathbf{k}_{2\text{D}} = 0$ point where $k_x = k_z = 0$, and is protected by time-reversal symmetry (see below). We emphasize the latter two nodes come from rotational symmetry along the k_z axis *in the bulk*. To see this, we note that at the two projected Dirac points $\pm\mathbf{k}^{\text{Dirac}}_{2\text{D}} = (k_x = 0, k_z = \pm k_0)$, the inverse decay length (see Eq. 20)

$$1/\lambda_{\mathbf{k}^{\text{Dirac}}_{2\text{D}}} = -m_{\mathbf{k}^{\text{Dirac}}_{2\text{D}}}/v = 0, \tag{27}$$

since $m^{\text{Dirac}}_{\mathbf{k}_{2\text{D}}}$ vanishes at the projected Dirac points. This means that the surface wavefunction delocalizes completely into the bulk since $1/\lambda_{\mathbf{k}^{\text{Dirac}}_{2\text{D}}}$ diverges at these projected Dirac points on the surface, $\pm\mathbf{k}^{\text{Dirac}}_{2\text{D}}$. As a result, $\Delta^{(0)}_{\mathbf{k}_{2\text{D}}}$ in Eq. (26) above (capturing the *intrinsic* coupling between spinors on a *perfect* surface) also vanishes at the pair of projected Dirac points due to rotational symmetry *in the bulk* (see also Ref. [14]).

However, surface potentials that couple the spin-blocks can also contribute to Eq. (25) yielding renormalized values of $\Delta_{\mathbf{k}_{2\text{D}}} = \Delta^{(0)}_{\mathbf{k}_{2\text{D}}} + \Delta'_{\mathbf{k}_{2\text{D}}}$, where $\Delta'_{\mathbf{k}_{2\text{D}}}$ arise from a surface potential V_{surf} mixes $\uparrow$ and $\downarrow$ spins on the Fermi arc states so that

$$\Delta'_{\mathbf{k}_{2\text{D}}} = \langle \Psi^{\text{surf}}_{\mathbf{k}_{2\text{D}}\uparrow} | V_{\text{surf}} | \Psi^{\text{surf}}_{\mathbf{k}_{2\text{D}}\downarrow} \rangle, \tag{28}$$

where

$$V_{\text{surf}} = \begin{pmatrix} 0 & V_{\uparrow\downarrow} \\ V^\dagger_{\uparrow\downarrow} & 0 \end{pmatrix}, \tag{29}$$

with $V_{ss'}$ $(s, s' = \uparrow, \downarrow)$ are 2×2 matrices. Importantly, we note that for V_{surf} that breaks rotational symmetry, $\Delta_{\mathbf{k}_{2\text{D}}}$ at $\pm\mathbf{k}^{\text{Dirac}}_{2\text{D}} = (k_x = 0, k_z = \pm k_0)$ may no longer vanish identically since this lifts the degeneracy of the two surface states at the projected Dirac nodes. However, for simplicity we will concentrate on V_{surf} that preserve rotational symmetry in the main text.

Crucially, non-time-reversal-breaking surface potentials cannot lift the Kramers degeneracy at the projected $\mathbf{k}_{2\text{D}} = 0$ point where $k_x = k_z = 0$ as noted previously by [2]. For the convenience of the reader, we reproduce this argument using the notation of this manuscript. We note that

$$\begin{aligned} \Delta(\mathbf{k}_{2\text{D}} = 0) =& \langle \Psi^{\text{surf}}_{\mathbf{k}_{2\text{D}}=0\uparrow} | \mathcal{H}(\mathbf{k}_{2\text{D}} = 0) + V_{\text{surf}} | \Psi^{\text{surf}}_{\mathbf{k}_{2\text{D}}=0\downarrow} \rangle \\ =& \langle \Psi^{\text{surf}}_{\mathbf{k}_{2\text{D}}=0\uparrow} | \mathcal{H}(\mathbf{k}_{2\text{D}} = 0) + V_{\text{surf}} | \Theta \Psi^{\text{surf}}_{\mathbf{k}_{2\text{D}}=0\uparrow} \rangle \\ =& \langle (-iKs^y) \Theta \Psi^{\text{surf}}_{\mathbf{k}_{2\text{D}}=0\uparrow} | \\ & [\mathcal{H}(\mathbf{k}_{2\text{D}} = 0) + V_{\text{surf}}]^* | (-iKs^y) \Psi^{\text{surf}}_{\mathbf{k}_{2\text{D}}=0\uparrow} \rangle \\ =& \langle \Theta^2 \Psi^{\text{surf}}_{\mathbf{k}_{2\text{D}}=0\uparrow} | \mathcal{H}(\mathbf{k}_{2\text{D}} = 0) + V_{\text{surf}} | \Theta \Psi^{\text{surf}}_{\mathbf{k}_{2\text{D}}=0\uparrow} \rangle \\ =& -\Delta(\mathbf{k}_{2\text{D}} = 0) = 0, \end{aligned} \tag{30}$$

where the inner product $\langle \cdot \rangle$ is defined in Eq. (22), and $\mathcal{H}(\mathbf{k}_{2\text{D}} = 0) \equiv \mathcal{H}(\mathbf{k}_{2\text{D}} = 0, ik_y \to \partial_y)$ [see replacement in Eq. (17)]. Note that in performing the inner product in Eq. (22), the full y-dependence of the surface state wavefunction is taken into account. During the above argument, we have used $[\Theta, \mathcal{H}(\Gamma) + V_{\text{surf}}] = 0$, and $\Theta = -iKs^y$ is the time-reversal operator where $s^y = (s^y)^\dagger$ acts on the real spin and K denotes complex conjugation. From the second line to the the third line, we noted that $\Delta(\Gamma)$ is real valued and took the complex conjugate of overall expression. Lastly, we also noted that the time-reversal operator squares as $\Theta^2 = -1$ (see fourth and fifth lines).

To capture the both the intrinsic and surface potential contributions to inter arc mixing, we use a minimal phenomenological model for $\Delta_{\mathbf{k}_{2\text{D}}}$ that respects both TRS and RS. Lastly, we comment, parenthetically, that surface potentials can also in-principle induce particle-hole asymmetric terms. However, these can depend sensitively on the surface termination and sample preparation, and are beyond the current scope of our work.

Optical conductivity when $\Delta_{\mathbf{k}^{\text{Dirac}}_{2\text{D}}} \neq 0$

As discussed in the main text and in the previous section, the degeneracy of the surface states close to the projected Dirac points can be lifted when surface potentials break rotational symmetry. These gap openings will lead to reduce interband conductivity discussed in the main text. To illustrate their effect, here we consider a small gap opening at the Dirac points Δ_D smaller than Δ_0. To mimic the gap opening at the projected Dirac points we use a modified sin model $\Delta_{\mathbf{k}_{2\text{D}}} = \Delta_0 \sin[\pi k_z/(k_0 + \delta k_0)]$,

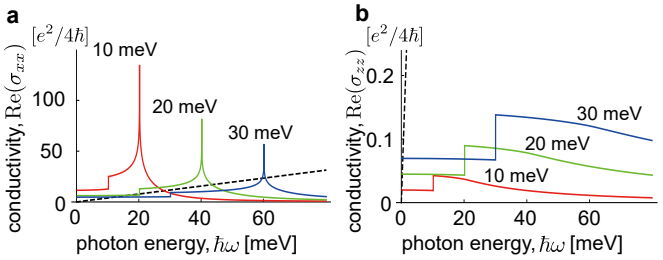

FIG. 4: Numerically calculated real part of interband conductivity $\mathrm{Re}(\sigma_{xx})$ [solid lines in (a)] and $\mathrm{Re}(\sigma_{zz})$ [solid lines in (b)] from inter Fermi arc state transitions at $\mu = 0$, with the gap opening $\Delta_D = \Delta_0/2$ at the Dirac points. Other parameters are used same as Fig. 2. The sharp steps occurring at $\hbar\omega = 2\Delta_D$ arise only at zero temperature $T = 0$. These will be smoothed out when the temperature $T > 0$.

which has gap openings $\Delta_D = \Delta_0[\pi k_0/(k_0 + \delta k_0)]$ at the Dirac points. We numerically calculate the interband conductivity using the correspondingly modified Eq. (6) and (7) in the main text as shown in Fig. 4. Importantly, we find that, when $\Delta_D < \Delta_0$, the transition between A- and B- type contours as well as the peak in $\mathrm{Re}(\sigma_{xx})$ will persist. Furthermore, since the gap opening will affect both $\mathrm{Re}(\sigma_{xx})$ and $\mathrm{Re}(\sigma_{zz})$ simultaneously, it will not alter the polarization anisotropy in the surface states.

Comparison of intrinsic model with $\Delta_{\mathbf{k}_{2D}} = \Delta^{(0)}_{\mathbf{k}_{2D}}$ and minimal model

In this section we compare the dispersion and spin texture obtained from the minimal model with that of intrinsic coupling between the spin sectors. For Cd_3As_2 (structure I) and A_3Bi (A=Na, K, Rb) Dirac semimetals, without considering the contributions of surface potentials, the intrinsic effective surface Hamiltonian reads as

$$\mathcal{H}_{\mathrm{surf},0} = vk_x\sigma_z + \Delta^{(0)}_{\mathbf{k}_{2D}}\sigma_x, \tag{31}$$

where $\Delta^{(0)}_{\mathbf{k}_{2D}} = \alpha k_z(k_x - 1/\lambda_{\mathbf{k}_{2D}})^2$ (see Eq. 25), and $\lambda_{\mathbf{k}_{2D}}$ is self-consistently determined by the equation $\lambda_{\mathbf{k}_{2D}} = -v/m_{\mathbf{k}_{2D}}$ with $m_{\mathbf{k}_{2D}} \to m(k_x, ik_y = -1/\lambda_{\mathbf{k}_{2D}}, k_z)$. For $m_{\mathbf{k}_{2D}} = -m_0 + m_1k_z^2 + m_2(k_x^2 + k_y^2)$,

$$\lambda_{\mathbf{k}_{2D}} = \frac{2m_2}{v - \sqrt{v^2 + 4m_2(-m_0 + m_1k_z^2 + m_2k_x^2)}}, \tag{32}$$

where v is the carrier velocity in the x-direction in the bulk (see Eq. 15). In Fig. 5, we show the dispersion of the intrinsic surface Hamiltonian [Fig. 5(a)], and its spin texture for A- [Fig. 5(c)] and B- [Fig. 5(e)] type equi-energy contours. Compared to the intrinsic model, one can see that the minimal sin model captures the qualitative features of the dispersion [Fig. 5(b)] as well as the spin texture [Fig. 5(d) and (f)] of the surface states quite well.

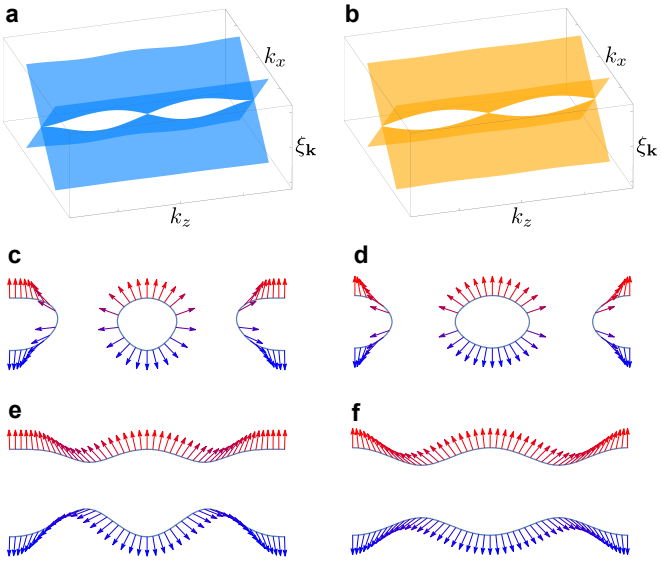

FIG. 5: (a) The dispersion of the intrinsic surface Hamiltonian $\Delta^{(0)}_{\mathbf{k}_{2D}} = \alpha k_z(k_x - 1/\lambda_{\mathbf{k}_{2D}})$, and (b) the dispersion of the sin model $\Delta_{\mathbf{k}_{2D}} = \Delta_0 \sin(\pi k_z/k_0)$, in which we have taken $\alpha = 7\Delta_0$ by hand to make the two models resembling to each other. Other parameters are used same as Fig. 2. (c) and (e) are spin textures for A- and B- type contours [see Fig. 1(b) in the main text] for intrinsic model, while (d) and (f) are for the sin model.

Jacobian factor for inter surface state transitions

The Jacobian factor in the main text [see Eq. (6)] are different for A-type and B-type contours. The idea is to avoid singularities by choosing different sets of parameters for A-type or B-type transitions.

In A-type contours, $\hbar\omega < 2\Delta_0$, the contours are disconnected segments and can be described by the parameter $\phi_{\mathbf{k}}$ which is continuous between $-\pi$ to π. In this case, we have

$$\sqrt{v^2k_x^2 + \Delta_0^2 \sin^2\frac{\pi k_z}{k_0}} = \eta, \quad \phi_{\mathbf{k}_{2D}} = \arctan\frac{\Delta_0 \sin\frac{\pi k_z}{k_0}}{vk_x}, \tag{33}$$

yielding

$$R = \left|\frac{\partial(k_x, k_z)}{\partial(\eta, \phi)}\right| = 2\frac{1}{(2\pi)^2}\frac{k_0}{\pi v}\frac{\eta}{\Delta_0}\frac{1}{[1 - (\eta/\Delta_0)^2 \sin^2\phi]^{1/2}}, \tag{34}$$

where a factor of 2 in the numerator comes from adding up contributions from the central circle, as well as the side circles (see Fig. 1b in the main text); In B-type contours, $\hbar\omega \geq 2\Delta_0$, the contours are two curves can be described by the parameter k_z which is continuous between $-k_0$ to k_0. In this case, we use another set of parameters (η, ν) where $\nu \in [-\pi, \pi]$:

$$\sqrt{v^2k_x^2 + \Delta_0^2 \sin^2\frac{\pi k_z}{k_0}} = \eta, \quad k_z = k_0\frac{\nu}{\pi}, \tag{35}$$

and arrive at

$$R = \left|\frac{\partial(k_x,k_z)}{\partial(\eta,\nu)}\right| = 2\frac{1}{(2\pi)^2}\frac{k_0}{\pi v}\frac{1}{[1-(\Delta_0/\eta)^2\sin^2\nu]^{1/2}}, \tag{36}$$

in which the factor of 2 results from summing over contributions from two singly-connected Fermi arcs (see Fig. 1b in the main text).

Optical conductivity of bulk states

Neglecting cubic terms, the 4×4 Dirac semimetal Hamiltonian (Eq. 15) has two non-interacting and time-reversal blocks, and each of them possesses a pair of Dirac nodes. We can pick one of the four Dirac nodes to calculate the optical response. Near the Dirac nodes $(0,0,k_0)$, where $k_0=\sqrt{m_0/m_1}$, the Hamiltonian can be simplified as

$$\mathcal{H}_\uparrow = (A_x k_x, -A_y k_y, A_z k_z), \tag{37}$$

where $A_x = A_y = v$, and $A_z = 2\sqrt{m_0 m_1}$. The eigenstate and energy for the 2×2 Hamiltonian are

$$\psi_{+\mathbf{k}}(\mathbf{r}) = \begin{pmatrix}\cos\frac{\theta_\mathbf{k}}{2}\\ \sin\frac{\theta_\mathbf{k}}{2}e^{i\phi_\mathbf{k}}\end{pmatrix}, \quad \psi_{-\mathbf{k}}(\mathbf{r}) = \begin{pmatrix}\sin\frac{\theta_\mathbf{k}}{2}\\ -\cos\frac{\theta_\mathbf{k}}{2}e^{i\phi_\mathbf{k}}\end{pmatrix}, \tag{38}$$

with

$$\tan\theta_\mathbf{k} = \frac{A_x}{A_z}\frac{\sqrt{k_x^2+k_y^2}}{k_z}, \quad \tan\phi_\mathbf{k} = -\frac{k_y}{k_x}, \tag{39}$$

and

$$\xi^\pm_\mathbf{k} = \pm\sqrt{A_x^2(k_x^2+k_y^2)+A_z^2k_z^2}, \tag{40}$$

where $\mathbf{k}=(k_x,k_y,k_z)$.

In the presence of incident light $\boldsymbol{\mathcal{E}} = \mathbf{E}\cos\omega t$, electron-hole transitions occur between the occupied bulk states and unoccupied bulk states. These can be described via the standard golden rule technique as

$$W_\uparrow = \frac{2\pi}{\hbar}\sum_\mathbf{k}|M_{\uparrow,\mathbf{k}}|^2\delta(\xi^+_\mathbf{k}-\xi^-_\mathbf{k}-\hbar\omega)\Theta(\hbar\omega-2|\mu|), \tag{41}$$

where $\Theta(\hbar\omega-2|\mu|)$ means that only when the energies of incident photons are greater than $|2\mu|$, which is the chemical potential counted from the Dirac nodes, the optical transitions are allowed.

Writing $\mathbf{k}\to\mathbf{k}-e\boldsymbol{\mathcal{A}}/\hbar c$ in the spin up Hamiltonian (Eq. 37), with the vector potential satisfying $\boldsymbol{\mathcal{A}} = (1/c)\partial_t\boldsymbol{\mathcal{E}}$, and expanding to linear order in $\mathbf{E}$ yields the matrix elements

$$|M_{\uparrow,\mathbf{k},i}|^2 = \left(\frac{ieA_iE_i}{2\hbar\omega}\right)^2|\langle\psi_{+\mathbf{k}}|\sigma^i|\psi_{-\mathbf{k}}\rangle|^2, \ (i=x,y,z). \tag{42}$$

Using the eigenstates given above, we have

$$\langle\psi_{+\mathbf{k}}|\sigma^x|\psi_{-\mathbf{k}}\rangle = \sin^2\frac{\theta_\mathbf{k}}{2}e^{-i\phi_\mathbf{k}} - \cos^2\frac{\theta_\mathbf{k}}{2}e^{i\phi_\mathbf{k}}, \tag{43}$$

$$\langle\psi_{+\mathbf{k}}|\sigma^y|\psi_{-\mathbf{k}}\rangle = i(\sin^2\frac{\theta_\mathbf{k}}{2}e^{-i\phi_\mathbf{k}} + \cos^2\frac{\theta_\mathbf{k}}{2}e^{i\phi_\mathbf{k}}), \tag{44}$$

and

$$\langle\psi_{+\mathbf{k}}|\sigma^z|\psi_{-\mathbf{k}}\rangle = \sin\theta_\mathbf{k}. \tag{45}$$

For linearly polarized light $\boldsymbol{\mathcal{E}} = E\hat{\mathbf{x}}$ ($\boldsymbol{\mathcal{E}} = E\hat{\mathbf{y}}$), it gives

$$|M_{\uparrow,\mathbf{k},x(y)}|^2 = \left(\frac{evE}{2\hbar\omega}\right)^2\left(\cos^2\theta_\mathbf{k}\cos^2\phi_\mathbf{k}+\sin^2\phi_\mathbf{k}\right), \tag{46}$$

The transition rates for both the Dirac nodes, $(0,0,\zeta k_0)$, are the same when they have the same chemical potential

$$\begin{aligned}W_{\uparrow,x(y)} =& \frac{2\pi}{\hbar}\left(\frac{evE}{2\hbar\omega}\right)^2\sum_\mathbf{k}\left(\cos^2\theta_\mathbf{k}\cos^2\phi_\mathbf{k}+\sin^2\phi_\mathbf{k}\right)\\ &\times\delta(\xi^+_\mathbf{k}-\xi^-_\mathbf{k}-\hbar\omega)\ \Theta(\hbar\omega-2|\mu|)\\ =& \frac{e^2}{\hbar}\frac{1}{48\pi}\frac{1}{A_z/L_z}L_xL_yE^2\ \Theta(\hbar\omega-2|\mu|).\end{aligned} \tag{47}$$

Using Ohm's law

$$\hbar\omega W_{\uparrow,x(y)} = \mathrm{Re}\,[\sigma^{\mathrm{bulk}}_{\uparrow,xx}(\omega)]E^2L_xL_y/2, \tag{48}$$

one has

$$\mathrm{Re}\,[\sigma^{\mathrm{bulk}}_{\uparrow,xx}(\omega)] = \frac{e^2}{\hbar}\frac{1}{12\pi}\frac{\hbar\omega}{A_z/L_z}\Theta(\hbar\omega-2|\mu|), \tag{49}$$

where we have summed over both two nodes.

Similarly one has

$$\mathrm{Re}\,[\sigma^{\mathrm{bulk}}_{\uparrow,zz}(\omega)] = \frac{e^2}{\hbar}\frac{1}{12\pi}\frac{\hbar\omega}{A_x^2/A_zL_y}\Theta(\hbar\omega-2|\mu|). \tag{50}$$

Useful identity involving $\mathcal{I}_x$ and I_x

During the calculation of interband conductivity described in the main text, the frequency dependence of interband conductivity arose from

$$I_x(\omega) = \frac{\bar\omega^{-\frac{3}{2}(1+\zeta)}}{4\pi}\int_{-\pi}^{\pi}(1-\bar\omega^{-2\zeta}\sin^2\nu)^{-\frac{1}{2}}\sin^2\nu d\nu, \tag{51}$$

where $\bar\omega = \omega/2\Delta_0$, $\zeta(\bar\omega) = \mathrm{sgn}\,(\bar\omega-1)$. Similarly, the intraband (Drude) conductivity exhibited chemical potential dependence in the form

$$\mathcal{I}_x(\mu) = \frac{\bar\mu^{(1-\zeta)/2}}{4\pi}\int_{-\pi}^{\pi}\frac{1-\bar\mu^{-(1+\zeta)}\sin^2\nu}{(1-\bar\mu^{-2\zeta}\sin^2\nu)^{1/2}}d\nu, \tag{52}$$

where $\bar{\mu} = \mu/\Delta_0$. In Eq. (52), the exponent ζ depends on the chemical potential as $\zeta(\bar{\mu}) = \mathrm{sgn}\,(\bar{\mu} - 1)$. We note that it will be useful to express both Eq. (51) and (52) in terms of the elliptic integrals of the first, and second kind, $K(x) = \int_0^{\pi/2}(1 - x\sin^2\phi)^{-1/2}d\phi$, and $E(x) = \int_0^{\pi/2}(1 - x\sin^2\phi)^{1/2}d\phi$ respectively [Note that here we define $K(x)$ and $E(x)$ in terms of the parameter $x = k^2$, where k is the elliptic modulus]:

$$I_x(\omega) = \frac{K(\bar{\omega}^{-2\zeta}) - E(\bar{\omega}^{-2\zeta})}{\pi\bar{\omega}^{\frac{1}{2}(3-\zeta)}}, \tag{53}$$

and

$$\mathcal{I}_x(\mu) = \frac{\bar{\mu}^{\zeta}E(\bar{\mu}^{-2\zeta}) - (-\bar{\mu} + \bar{\mu}^{\zeta})K(\bar{\mu}^{-2\zeta})}{\pi\bar{\mu}^{\frac{1}{2}(1+\zeta)}}. \tag{54}$$

When $\zeta = \pm 1$, and by directly taking a derivative, we find

$$\partial_{\bar{\mu}}\mathcal{I}_x(\mu) = \frac{K(\bar{\mu}^{-2\zeta}) - E(\bar{\mu}^{-2\zeta})}{\pi\bar{\mu}^{\frac{1}{2}(3-\zeta)}}, \tag{55}$$

In obtaining Eq. (55) we have used the identities $dK(x)/dx = E(x)/2x(1-x) - K(x)/2x$, $dE(x)/dx = [E(x) - K(x)]/2x$ Using $\partial_\mu = \Delta_0^{-1}\partial_{\bar{\mu}}$, and comparing Eq. (55) with Eq. (53) we have

$$\partial_\mu\mathcal{I}_x(\mu) = \Delta_0^{-1}I_x(2\mu), \tag{56}$$

where we have made the replacement of $\omega = 2\mu$ in the final line.